

$$\left[\frac{\nu_x^2}{-1} \frac{S_\xi^{*2}}{I_\xi^* M_x^*} \right]$$

$\leq 1/\text{rev}$. The solution near $\omega =$

$$\left[\frac{S_\xi^{*2}}{I_\xi^* M_y^* M_x^*} \right]$$

ion, and also for the $\omega = \nu_\xi - 1$ limit $\omega = 0$, for which the characteristic equation gives $\nu_\xi - 1 = 0$. With this solution defines where the roots cross the ω -axis. The speed for which $\nu_\xi = 1/\text{rev}$. In the limit $\omega \rightarrow -1$ that intercepts the Ω -axis is the low frequency lag mode root for all values of S_ξ .

In the case of no damping can be presented in a Coleman diagram, which is a plot of the roots of the characteristic equation (dimensional solution for the uncoupled rotor ν_ξ , plus the corresponding negative solutions for ω (The negative solutions for ω are not plotted.) based on the above results for $\Omega = 0$ and $\Omega = \infty$, plus the knowledge that the roots never cross. The character of the solution depends on the lag frequency $\nu_\xi^2 = 1/\text{rev}^2$. Figs. 12-12 and 12-13 present the Coleman diagram for an articulated rotor ($K_1 = 0$ and $K_2 < 1$), and a stiff in-plane hingeless rotor ($K_2 < 1$), and a stiff in-plane hingeless rotor. The uncoupled solutions are sketches of typical results for hingeless rotors. The uncoupled solutions are horizontal lines at $\omega = \omega_x$ and $\omega = \omega_y$. For the articulated rotor are the low and high frequency modes. The approach $\nu_{NR} = \sqrt{K_1}$ at low

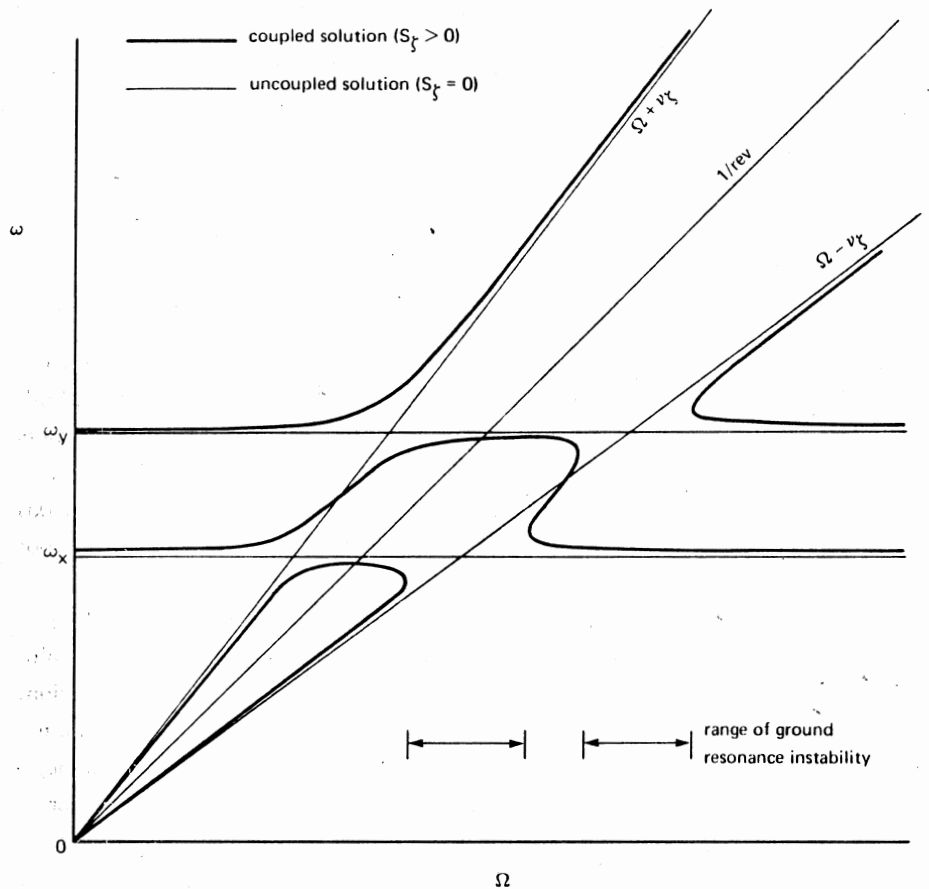


Figure 12-11 Coleman diagram of the ground resonance solution for an articulated rotor.

rotor speed and are asymptotic to constant per-rev values ($\sqrt{K_2} \pm 1/\text{rev}$) at high rotor speed. Thus the lag mode frequencies are in resonance with the support mode frequencies at some rotor speed.

For $S_\xi > 0$, the solution is displaced from the uncoupled frequencies, as indicated by the results for small coupling. If there are four positive solutions for ω at a given rotor speed, then the system is stable (neutrally stable for this case of zero damping). For the articulated and soft in-plane hingeless rotors (Figs. 12-11 and 12-12), however, there are ranges of Ω where only two positive real solutions for ω exist, occurring around the

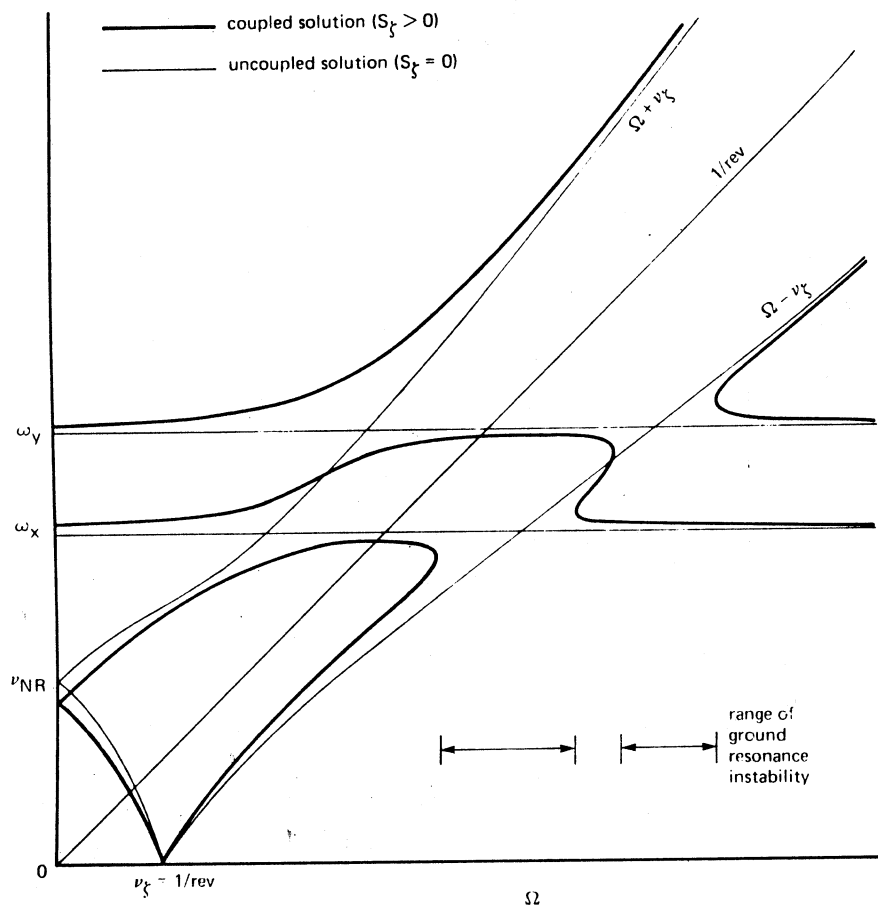
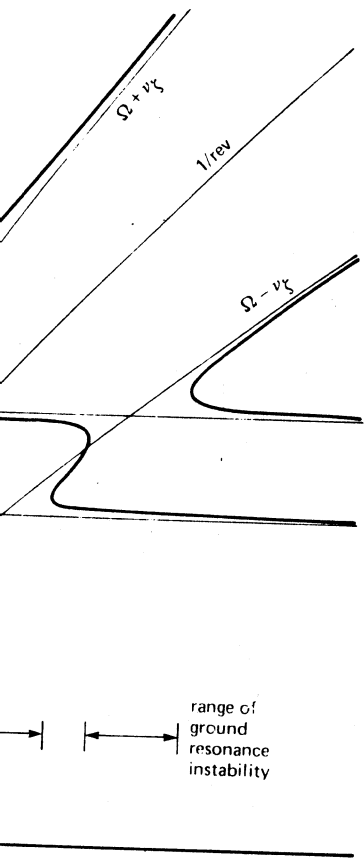


Figure 12-12 Coleman diagram of the ground resonance solution for a soft in-plane hingeless rotor.

resonances of the low frequency lag mode ($\Omega - \nu_\zeta$) with a support mode (ω_x or ω_y). The characteristic equation has four complex solutions in these ranges, so the system is unstable. For the stiff in-plane hingeless rotor (Fig. 12-13), four positive solutions for ω exist at all rotor speeds, and a ground resonance instability does not occur. This behavior of the ground resonance solution is determined by the direction the roots are shifted when $S_\zeta > 0$, which depends on whether $\nu_\zeta < 1/\text{rev}$ or $\nu_\zeta > 1/\text{rev}$ at the resonance of the low frequency lag mode with a support mode.



resonance solution for a soft

$-\nu_\zeta$) with a support mode
 four complex solutions in
 the stiff in-plane hingeless
 ω exist at all rotor speeds,
 occur. This behavior of the
 the direction the roots are
 $\nu_\zeta < 1/\text{rev}$ or $\nu_\zeta > 1/\text{rev}$
 mode with a support mode.

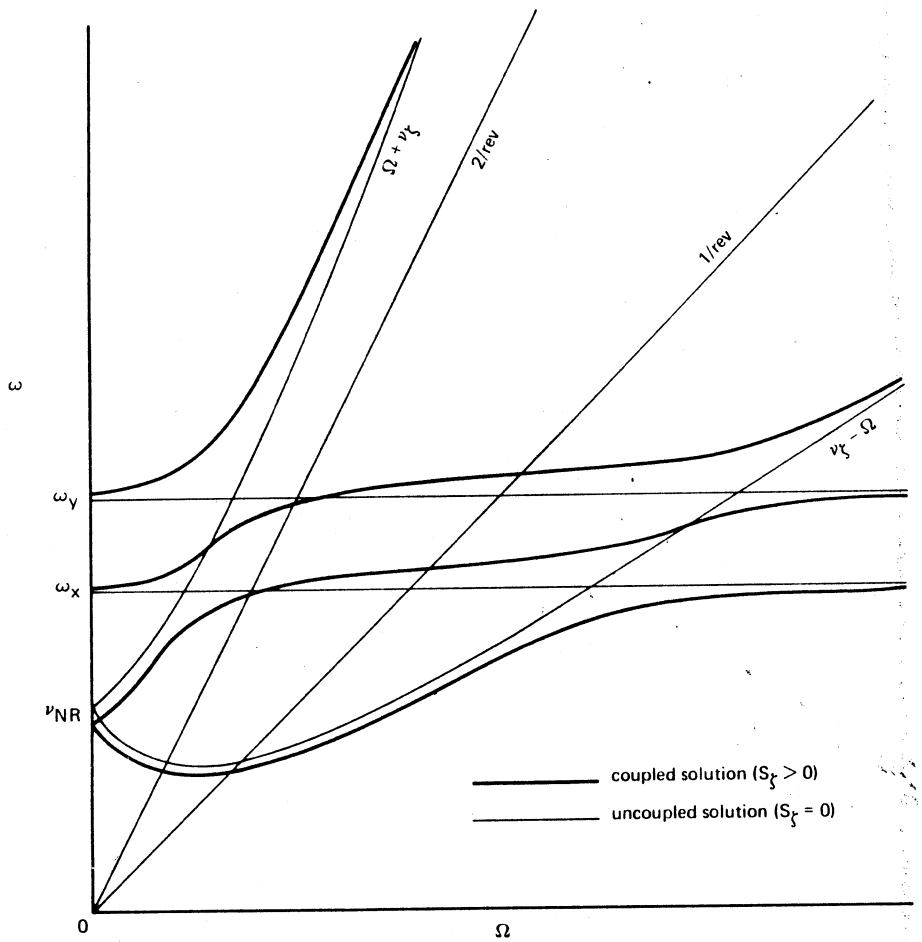


Figure 12-13 Coleman diagram of the ground resonance solution for a stiff in-plane hingeless rotor.

In conclusion, a ground resonance instability can occur at a resonance of a rotor mode and a support mode. The resonances of the high frequency lag mode ($\omega = 1 + \nu_\zeta$) are always stable, but resonances of the low frequency lag mode ($\omega = 1 - \nu_\zeta$) will be unstable if the rotating natural frequency ν_ζ is below $1/\text{rev}$, as for articulated and soft in-plane hingeless rotors. Thus the placement of the rotor lag frequency determines whether or not a ground resonance instability can occur.

$$\begin{bmatrix} \xi_1 \\ y_r \\ x_r \end{bmatrix} = 0$$

olis and centrifugal forces
The characteristic equation

$$s^2 + C_\xi^* s + \nu_\xi^2) \\ 4s(s^2 - 1)(2s + C_Y^*) = 0$$

tion reduces to

$$-8s^2(s^2 - 1) = 0$$

, where $\omega = \nu_\xi$ and $\omega =$
in the rotating frame are
rotating frame, and the

tic equation for the case
coupled solution. Writing
obtain

$$[-8\nu_\xi^2(\nu_\xi^2 + 1) \frac{S_\xi^{*2}}{I_\xi^* M_Y^*}]$$

$$\frac{S_\xi^{*2}}{I_\xi^* M_Y^*}]$$

s shift when $S_\xi > 0$ can
hing infinity. At $\Omega = 0,$
and that the larger root
hen Ω is large, of the

three roots corresponding to $\omega = \nu_\xi$ and $\omega_\gamma \pm 1$ the largest and smallest are increased, while the middle root is decreased. From this behavior the solution for $S_\xi > 0$ can be sketched. Figs. 12-14 and 12-15 present typical Coleman diagrams for articulated (soft in-plane) and stiff in-plane two-bladed rotors. As in the case of three or more blades, a ground resonance instability appears with soft in-plane rotors ($\nu_\xi < 1/\text{rev}$) at the resonance of the support and the low frequency lag mode - which in the rotating frame means $\nu_\xi = \Omega - \omega_\gamma$.

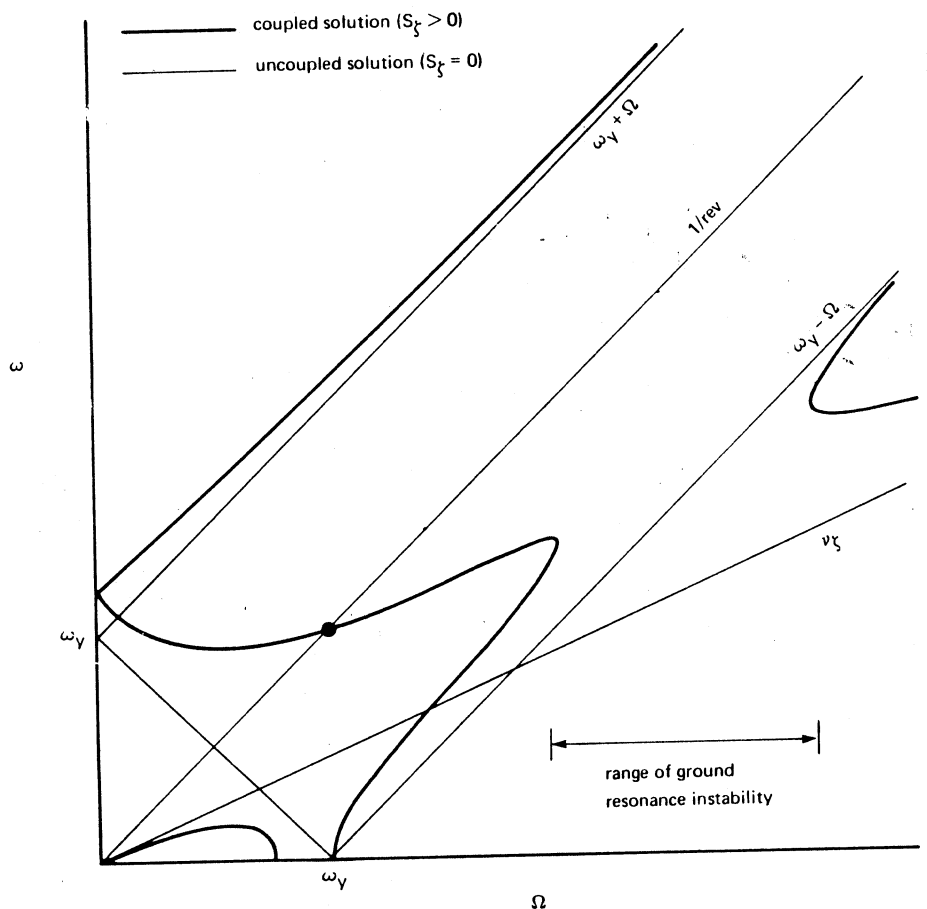


Figure 12-14 Coleman diagram of the ground resonance solution for a two-bladed articulated rotor ($\nu_\xi < 1/\text{rev}$) on an isotropic support.

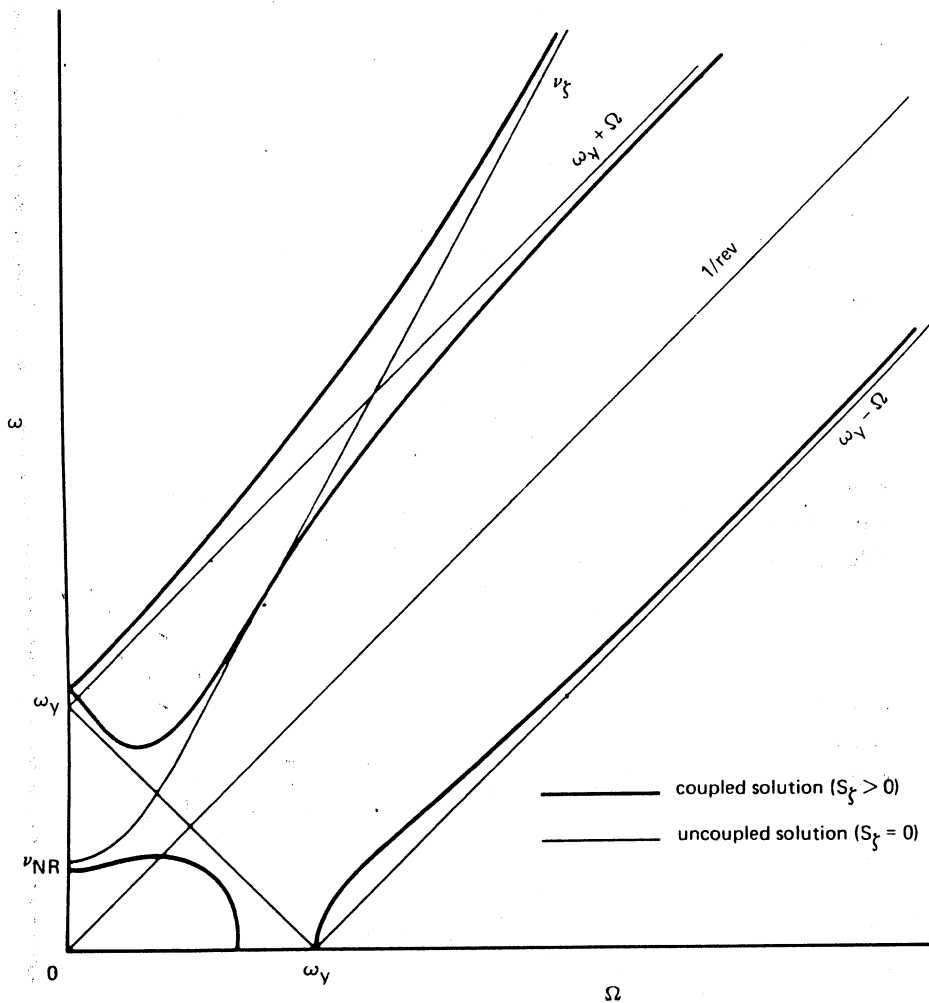


Figure 12-15 Coleman diagram of the ground resonance solution for a two-bladed stiff in-plane rotor ($\nu_\xi > 1/\text{rev}$) on an isotropic support.

Note that for $N = 2$ the center of the ground resonance instability range is shifted to a rotor speed above the uncoupled resonance, in contrast to the $N \geq 3$ case, for which the instability range remains centered about the resonance. This suggests that for large enough coupling the instability region might be shifted above the rotor operating range. To examine this

possibility of a resonance line, as indicated by the equation below.

Now since $\nu_\xi = 2/\text{rev}$ in this case and $\omega_y = \Omega$, the region of interest here is for rotor speeds

which include the instability range. This provides a condition

then both the uncoupled and coupled solutions show instability rather than stability. In the limit of zero coupling, the effect, seen in Figure 12-15, is

In Figure 12-15, only two modes are shown. The phenomenon of ground resonance has not been observed in the region of zero frequency for a rotating wing. This instability is not observed at zero rotor speed.